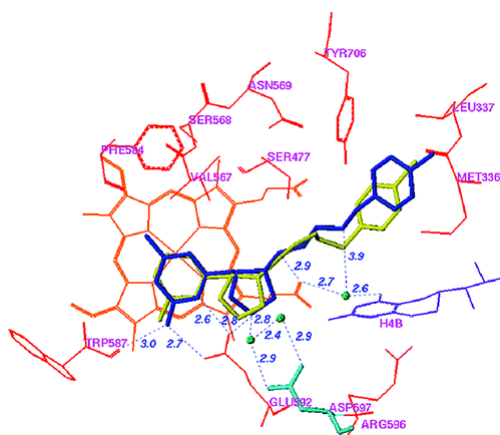


Silverman, R. B. *Acc. Chem. Res.* **2009**, *42*, 439-451.

Abstract:

2



Nitric oxide (NO), which is produced from L-arginine by the nitric oxide synthase (NOS) family of enzymes, is an important second-messenger molecule that regulates several physiological functions. In endothelial cells, it relaxes smooth muscle, which decreases blood pressure. Macrophage cells produce NO as an immune defense system to destroy pathogens and microorganisms. In neuronal cells, NO controls the release of neurotransmitters and is involved in synaptogenesis, synaptic plasticity, memory function, and neuroendocrine secretion.

NO is a free radical that is commonly thought to contribute to oxidative damage and molecule and tissue destruction, and thus it is somewhat surprising that it has so many significant beneficial physiological effects. However, the cell is generally protected from NO's toxic effects, except under certain pathological conditions in which excessive NO is produced. In that case, tissue damage and oxidative stress can result, leading to a wide variety of diseases, including rheumatoid arthritis, Alzheimer's disease, and Parkinson's disease, among others. In this Account, we describe research aimed at identifying small molecules that can selectively inhibit only the neuronal isozyme of NOS, nNOS. By targeting only nNOS, we attained the beneficial effects of lowering excess NO in the brain without the detrimental effects of inhibition of the two isozymes found elsewhere in the body (eNOS and iNOS).

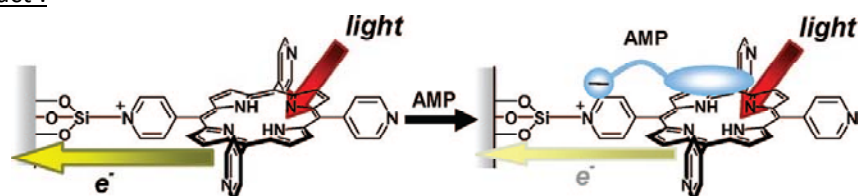
Initially, in pursuit of this goal, we sought to identify differences in the second sphere of amino acids in the active site of the isozymes. From this study, the first class of dual nNOS-selective inhibitors was identified. The moieties important for selectivity in the best lead compound were determined by structure modification. Enhancement provided highly potent, nNOS-selective dipeptide amides and peptidomimetics, which were active in a rabbit model for fetal neurodegeneration. Crystal structures of these compounds bound to NOS isozymes showed a one-amino-acid difference between nNOS and eNOS in the second sphere of amino acids; this was the difference that we were searching for from the beginning of this project. With the aid of these crystal structures, we developed a new fragment-based *de novo* design method called "fragment hopping", which allowed the design of a new class of nonpeptide nNOS-selective inhibitors. These compounds were modified to give low nanomolar, highly dual-selective nNOS inhibitors, which we recently showed are active in a rabbit model for the prevention of neurobehavioral symptoms of cerebral palsy. These compounds could also have general application in other neurodegenerative diseases for which excess NO is responsible.

- Photoelectrochemical Sensor with Porphyrin-Deposited Electrodes for Determination of Nucleotides in Water

3

Ikeda, A.; Nakasu, M.; Ogasawara, S.; Nakanishi, H.; Nakamura, M.; Kikuchi, J. *Org. Lett.* **2009**, *11*, 1163-1166.

Abstract :

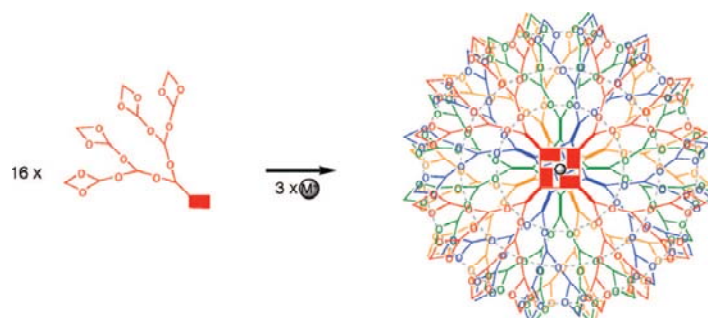


A 5,10,15,20-tetra(4-pyridyl)porphyrin (TPyP)-deposited ITO electrode as a sensor of nucleotides using photocurrent change was prepared. The TPyP-deposited ITO electrode could repeatedly detect nucleotides having concentrations of the μM order by a decrease in the photocurrent.

- Hexadecameric Self-Assembled Dendrimers Built from 2'-Deoxyguanosine Derivatives

Betancourt, J. E.; Rivera, J. M. *Org. Lett.* **2008**, *10*, 2287-2290.

Abstract :

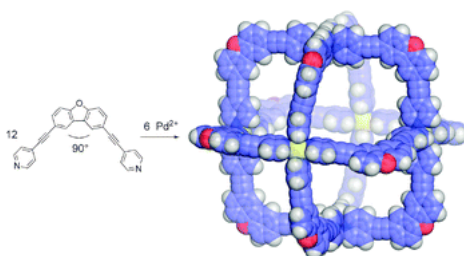


Herein we describe the construction of hexadecameric self-assembled dendrimers (SADs) using a series of dendronized 8-(*m*-acetylphenyl)-2'-deoxyguanosine (mAG) subunits. The azido-substituted mAG subunits were covalently linked to alkynyl polyester dendrons using a copper-catalyzed 1,3-dipolar cycloaddition reaction. Discrete SADs are formed with high fidelity and thermal stability even with the increased steric hindrance offered by the dendrons.

- Self-assembly of an M_6L_{12} coordination cube.

Suzuki, K.; Tominaga, M.; Kawano, M.; Fujita, M. *Chem. Commun.* **2009**, 1638 – 1640.

Abstract :



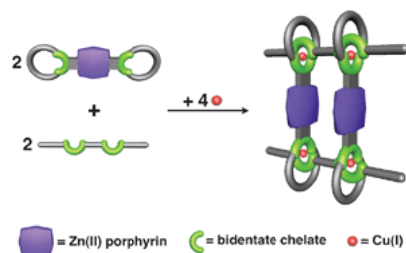
A $3 \times 3 \times 3$ nm cubic coordination compound quantitatively self-assembled from 6 palladium ions and 12 bent ligands with a 90° bend angle.

- Quantitative formation of [4]pseudorotaxanes from two rods and two bis-macrocycles incorporating porphyrinic plates between the rings.

Collin, J. P.; Durola, F.; Frey, J.; Heitz, V.; Sauvage, J.-P.; Tock C.; Trolez, Y. *Chem. Commun.* **2009**, 1706 – 1708.

4

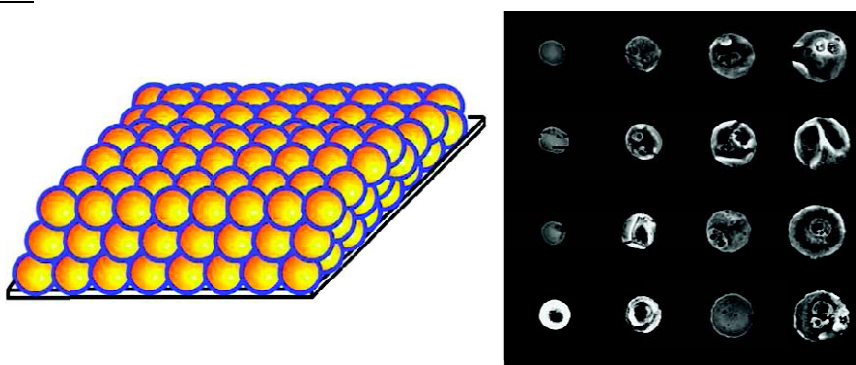
Abstract :



[4]Pseudorotaxanes consisting of two very large coordinating bis-macrocycles and rigid rods incorporating two side-by-side chelates have been obtained quantitatively utilising the gathering and threading effect of copper(I); the assemblies obtained are several nanometres long and they contain two face-to-face zinc porphyrins which will be used to complex various organic substrates.

- Nanoparticle-Based Solution Deposition of Gold Films Supporting Bioresistant SAMs
Kowalczyk, B.; Byrska, M.; Mahmud, G.; Huda, S.; Kandere-Grzybowska, K.; Grzybowski, B. A. *Langmuir* **2009**, *25*, 1905-1907.

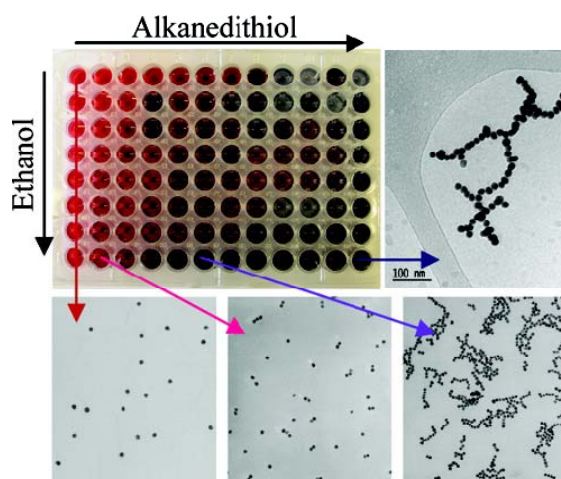
Abstract:



Thin films of gold on glass are prepared by solution deposition of functionalized gold nanoparticles followed by thermal treatment. The processed films adhere strongly to glass without any adhesion layers and can be micropatterned/ microetched without delamination from the substrate. The formation of self-assembled monolayers (SAMs) of oligo(ethylene glycol) alkane thiols (EG SAMs) renders the films resistant to cell adhesion and allows for cell patterning.

- Controlled Step Growth of Molecularly Linked Gold Nanoparticles: From Metallic Monomers to Dimers to Polymeric Nanoparticle Chains
Hussain, I.; Brust, M.; Barauskas, J.; Cooper, A. I. *Langmuir* **2009**, *25*, 1934-1939.

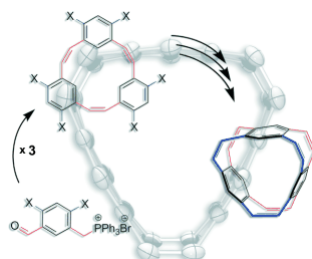
Abstract:



The solution-phase assembly of 15 nm gold particles into relatively linear chains of fairly controllable length of up to 1 μm is achieved by molecularly linking nanoparticles with alkanedithiols. This step-growth process can be controlled to prepare dimers, oligomers, and polymer-like gold nanoparticle chains by varying the ratio of alkanedithiols to nanoparticles. These size-controlled, relatively linear aggregates remain suspended in ethanol solution without precipitation for several weeks to months depending on the chain length. The resulting soluble nanoparticle assemblies were characterized by a variety of techniques including cryogenic transmission electron microscopy. The surface plasmon coupling of regularly spaced gold nanoparticles in these chains could be of interest in the fabrication of optical waveguide and nanoelectronic systems.

- From Metacyclophanes to Cyclacenes: Synthesis and Properties of $[6.8]_3$ Cyclacene
Esser, B.; Bandyopadhyay, A.; Rominger, F.; Gleiter, R. *Chem. Eur. J.* **2009**, *15*, 3368-3379.

Abstract:



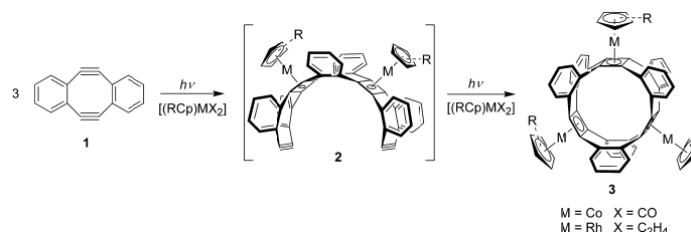
Conjugated belts: $[6.8]_3$ cyclacene as the first hydrocarbon cyclacene was synthesized in a de novo strategy. Various $[2_3]$ metacyclophanes are described as intermediates. The synthetic approach was extended to larger cyclacenes, and $[2_4]$ metacyclophanes as precursors of $[6.8]_4$ cyclacene were synthesized. In this article we show synthetic pathways to $[6.8]_n$ cyclacenes demonstrated by the de novo synthesis of $[6.8]_3$ cyclacene as the first purely hydrocarbon cyclacene and of precursors for $[6.8]_4$ cyclacene. The design of the de novo synthesis by exploring alternative pathways is discussed and various precursors are shown. Crucial to the synthesis of $[6.8]_3$ cyclacene were two cyclization steps. The first is a Wittig trimerization reaction which yielded the hexamethyl substituted *all-cis*- $[2_3]$ metacyclophanetriene. For the second cyclization step the methyl groups were converted to aldehyde functionalities by two subsequent oxidation steps of N-bromosuccinimide (NBS) bromination and oxidation with 2-iodoxybenzoic acid (IBX). The final cyclization of the second set of double bonds was achieved by a McMurry-coupling reaction. Towards the synthesis of $[6.8]_4$ cyclacene different synthetic pathways to methyl substituted *all-cis*- $[2_4]$ metacyclophanetetraenes were explored. Insights into the structures of $[2_3]$ metacyclophanetri-

and [2₄]metacyclophanetetraenes were gained by X-ray crystallographic investigations on various intermediates. A crystallographic analysis of [6.8]₃cyclacene revealed a *D*_{3h} symmetrical structure with planar benzene rings and a formation of tubular structures in the solid state.

- Synthesis, Properties and Formation of (RCp)Co- and (RCp)Rh-Stabilized[4.8]₃Cyclacene Derivatives

Kornmayer, S. C.; Hellbach, B.; Rominger, F.; Gleiter, R. *Chem. Eur. J.* **2009**, *15*, 3380-3389.

Abstract:

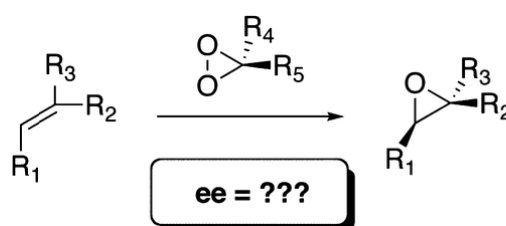


Metal-stabilized belts: A torus, **3**, consisting of three four- and three eight-membered conjugated rings and stabilized by (RCp)Co- and (RCp)Rh- units, was generated by irradiation of [(RCp)Co(CO)₂] and [(RCp)Rh(C₂H₄)₂], respectively, and **1**.

Eleven metal stabilized [4.8]₃cyclacene derivatives were synthesized. The substances were prepared in one-pot reactions by irradiation of a solution of 5,6,11,12-tetrahydrodibenzo[*a,e*]cyclooctatetraene and the corresponding cobalt reagents or rhodium compounds. The resulting cyclacene derivatives reveal *D*_{3h} symmetry in solution. In the solid state the hoop shaped systems crystallize in layers, which are intercalated with solvent layers. To unravel the mechanism of the one-pot reaction we isolated an intermediate, which shows almost planar cyclooctatetraene rings.

- Quantitative DFT Modeling of the Enantiomeric Excess for Dioxirane-Catalyzed Epoxidations
Schneebeli, S. T.; Hall, M. L.; Breslow, R.; Friesner, R. *J. Am. Chem. Soc.* **2009**, *131*, 3965–3973.

Abstract:



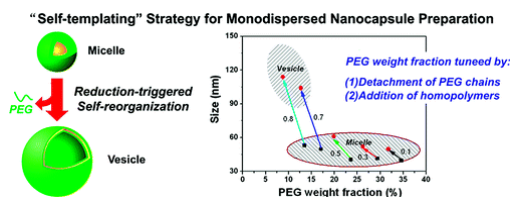
Herein we report the first fully quantum mechanical study of enantioselectivity for a large data set. We show that transition state modeling at the UB3LYP-DFT/6-31G* level of theory can accurately model enantioselectivity for various dioxirane-catalyzed asymmetric epoxidations. All the synthetically useful high selectivities are successfully “predicted” by this method. Our results hint at the utility of this method to further model other asymmetric reactions and facilitate the discovery process for the experimental organic chemist. Our work suggests the possibility of using computational methods not simply to explain organic phenomena, but also to predict them quantitatively.

- Monodispersed Polymeric Nanocapsules: Spontaneous Evolution and Morphology Transition from Reducible Hetero-PEG PICmicelles by Controlled Degradation

Dong, W. F.; Kishimura, A.; Anraku, Y.; Chuanoi, S.; Kataoka, K. *J. Am. Chem. Soc.* **2009**, *131*, 3804–3805.

7

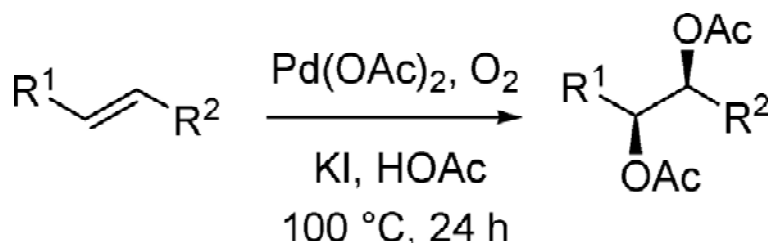
Abstract:



In this communication, a novel “self-templating” strategy was used to prepare uniform and biocompatible nanocapsules by the addition of a reduction agent (i.e., DTT) into a solution of highly monodispersed PICmicelles bearing a heterodetachable PEG corona. PEG chains were released from PICmicelle shells following disulfide reduction which leads a spontaneous and drastic morphology evolution from micelles to vesicles induced by the decrease of the PEG weight fraction. Formation of uniform nanocapsules with controllable capsule size was achieved by careful control of the micelle composition and molecular weight of homo-P[Asp(DET)].

- Palladium-Catalyzed Diacetoxylation of Alkenes with Molecular Oxygen as Sole Oxidant
Wang, A.; Jiang, H.; Chen, H. *J. Am. Chem. Soc.* **2009**, *131*, 3846–3847.

Abstract:

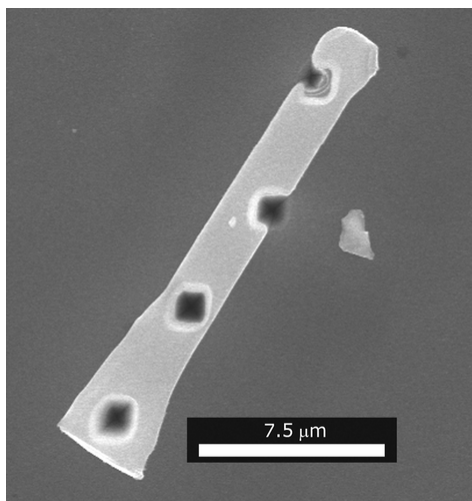


$\text{R}^1, \text{R}^2 = \text{alkyl, aryl, COOMe, CN}$

A new palladium-catalyzed diacetoxylation of alkenes using oxygen as the sole oxidant to afford diacetates was developed. High levels of diastereoselectivity in diacetoxylation of 1,2-disubstituted alkenes was obtained.

- Secondary Ion Mass Spectrometry of Vapor–Liquid–Solid Grown, Au-Catalyzed, Si Wires
Putnam, M. C.; Filler, M. A.; Kayes, B. M.; Kelzenberg, M. D.; Guan, Y.; Lewis, N. S.; Eiler, J. M.; Atwater, H. A. *Nano Lett.* **2008**, *8*, 3109–3113.

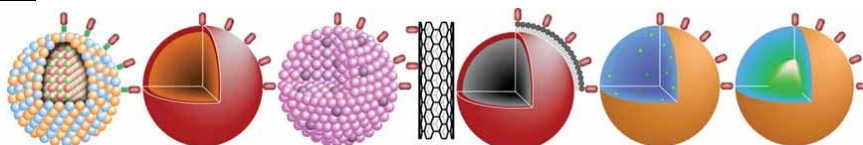
Abstract:



Knowledge of the catalyst concentration within vapor–liquid–solid (VLS) grown semiconductor wires is needed in order to assess potential limits to electrical and optical device performance imposed by the VLS growth mechanism. We report herein the use of secondary ion mass spectrometry to characterize the Au catalyst concentration within individual, VLS-grown, Si wires. For Si wires grown by chemical vapor deposition from SiCl_4 at 1000 °C, an upper limit on the bulk Au concentration was observed to be 1.7×10^{16} atoms/cm³, similar to the thermodynamic equilibrium concentration at the growth temperature. However, a higher concentration of Au was observed on the sidewalls of the wires.

- Nanoparticles for Optical Molecular Imaging of Atherosclerosis
 Douma, K.; Prinzen, L.; Slaaf, D. W.; Reutelingsperger, C. P. M.; Biessen, E. A. L.; Hackeng, T. M.; Post, M. J.; van Zandvoort, M. A. M. *J. Small* **2009**, 5, 544 – 557.

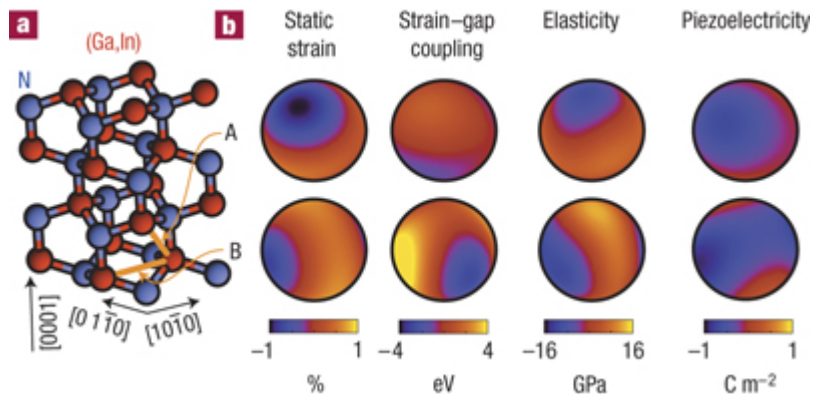
Abstract:



Molecular imaging contributes to future personalized medicine dedicated to the treatment of cardiovascular disease, the leading cause of mortality in industrialized countries. Endoscope-compatible optical imaging techniques would offer a stand-alone alternative and high spatial resolution validation technique to clinically accepted imaging techniques in the (intravascular) assessment of vulnerable atherosclerotic lesions, which are predisposed to initiate acute clinical events. Efficient optical visualization of molecular epitopes specific for vulnerable atherosclerotic lesions requires targeting of high-quality optical-contrast-enhancing particles. In this review, we provide an overview of both current optical nanoparticles and targeting ligands for optical molecular imaging of atherosclerotic lesions and speculate on their applicability in the clinical setting.

- A complete representation of structure–property relationships in crystals
 A. van de Walle *Nature Materials* **2008**, 7, 455-458.

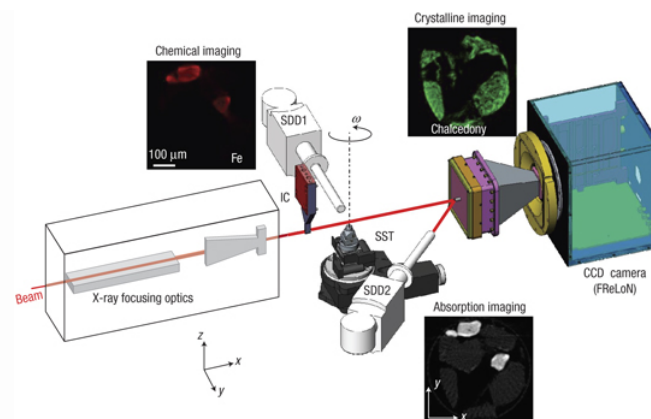
Abstract:



Whereas structure–property relationships have long guided the discovery and optimization of novel materials, formal quantitative methods to identify such relationships in crystalline systems are beginning to emerge. Among them is cluster expansion, which has been successfully used to parametrize the configurational dependence of important scalar physical properties such as bandgaps, Curie temperatures, equation-of-state parameters and densities of states. However, cluster expansion is currently unable to handle anisotropic properties, a key distinguishing feature of crystalline systems central to the design of modern epitaxial structures and devices. Here, I introduce a tensorial cluster expansion enabling the prediction of fundamental tensor-valued material properties such as elasticity, piezoelectricity, dielectric constants, optoelectric coupling, anisotropic diffusion coefficients, surface energy and stress. As an application, I develop predictive ab initio models of anisotropic properties relevant to the design and optimization of III–V semiconductor epitaxial optoelectronic devices.

- Probing the structure of heterogeneous diluted materials by diffraction tomography
Bleuet, P.; Welcomme, E.; Dooryhée, E.; Susini, J.; Hodeau, J.-L.; Walter, P. *Nature Materials* **2008**, 7, 468-472.

Abstract:

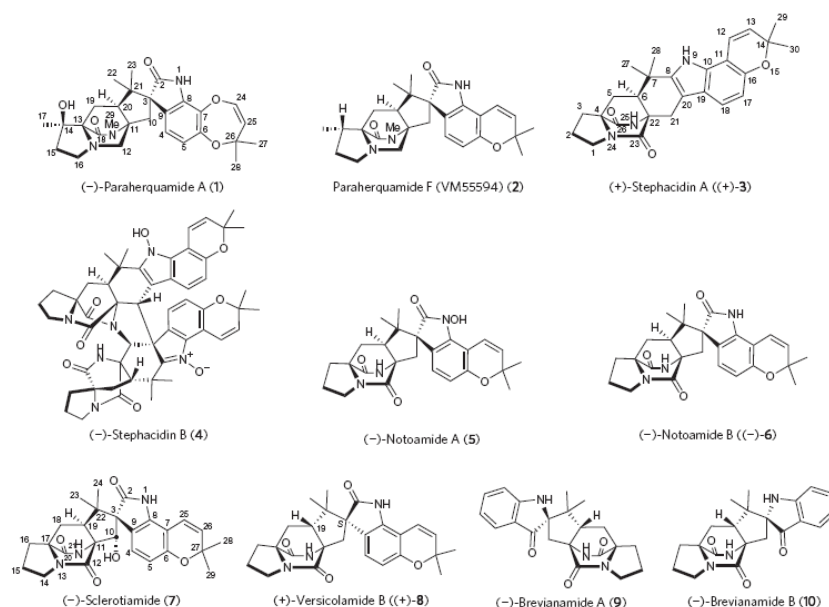


The advent of nanosciences calls for the development of local structural probes, in particular to characterize ill-ordered or heterogeneous materials. Furthermore, because materials properties are often related to their heterogeneity and the hierarchical arrangement of their structure, different structural probes covering a wide range of scales are required. X-ray diffraction is one of the prime structural methods but suffers from a relatively poor detection limit, whereas transmission electron analysis involves destructive sample preparation. Here we show the potential of coupling pencil-beam tomography with X-ray diffraction to examine unidentified phases in nanomaterials and polycrystalline materials. The demonstration is carried out on a high-pressure pellet containing

several carbon phases and on a heterogeneous powder containing chalcedony and iron pigments. The present method enables a non-invasive structural refinement with a weight sensitivity of one part per thousand. It enables the extraction of the scattering patterns of amorphous and crystalline compounds with similar atomic densities and compositions. Furthermore, such a diffraction-tomography experiment can be carried out simultaneously with X-ray fluorescence, Compton and absorption tomographies, enabling a multimodal analysis of prime importance in materials science, chemistry, geology, environmental science, medical science, palaeontology and cultural heritage.

- Asymmetric total syntheses of (1)- and (2)-versicolamide B and biosynthetic implications
Miller, K. A.; Tsukamoto, S.; Williams, R. M. *Nature Chemistry* **2009**, *1*, 63 – 68.

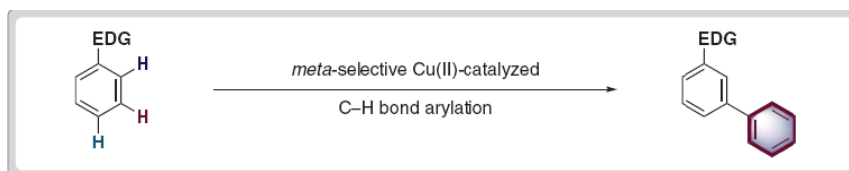
Abstract:



The Diels–Alder reaction is one of the most well-studied, synthetically useful organic transformations. Although it has been postulated that a significant number of naturally occurring substances arise by biosynthetic Diels–Alder reactions, rigorous confirmation of a mechanistically distinct natural Diels–Alderase enzyme remains elusive. Within this context, several related fungi within the *Aspergillus* genus produce a number of metabolites of opposite absolute configuration, including (1)- or (2)-versicolamide B. These alkaloids are hypothesized to arise via biosynthetic Diels–Alder reactions, implying that each *Aspergillus* species possesses enantiomerically distinct Diels–Alderases. In this paper, experimental validation of these biosynthetic proposals via deployment of the intramolecular hetero-Diels–Alder reaction as a key step in the asymmetric total syntheses of (1)- and (2)-versicolamide B is described. Laboratory validation of the proposed biosynthetic Diels–Alder construction, coupled with the secondary metabolite profile of the producing fungi, reveals that each *Aspergillus* species has evolved enantiomerically distinct indole oxidases, as well as enantiomerically distinct Diels–Alderases.

- A Meta-Selective Copper-Catalyzed C–H Bond Arylation
Phipps, R. J.; Gaunt, M. J. *Science* **2009**, *323*, 1593-1597.

Abstract:

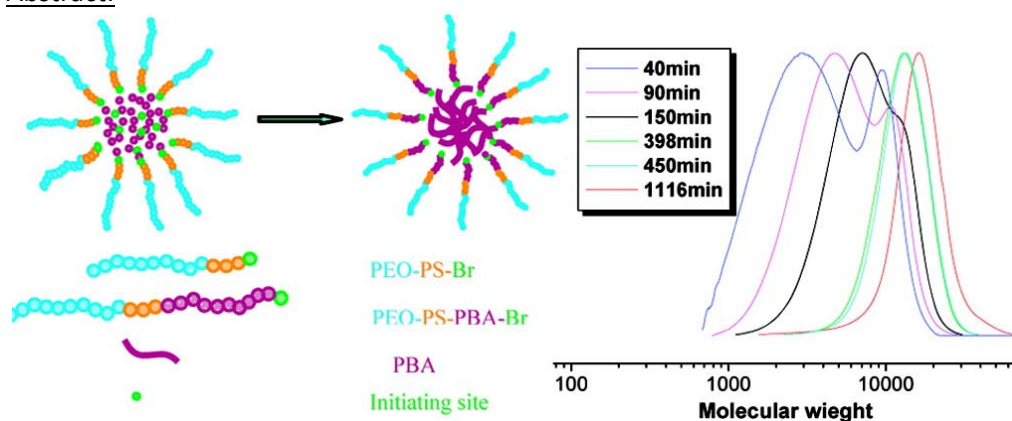


For over a century, chemical transformations of benzene derivatives have been guided by the high selectivity for electrophilic attack at the ortho/para positions in electron-rich substrates and at the meta position in electron-deficient molecules. We have developed a copper-catalyzed arylation reaction that, in contrast, selectively substitutes phenyl electrophiles at the aromatic carbon-hydrogen sites meta to an amido substituent. This previously elusive class of transformation is applicable to a broad range of aromatic compounds.

- PEO-Based Block Copolymers and Homopolymers as Reactive Surfactants for AGET ATRP of Butyl Acrylate in Miniemulsion.

Li, W.; Min, K.; Matyjaszewski, K.; Stoffelbach, F.; Charleux, B. *Macromolecules* **2008**, *41*, 6387-6392.

Abstract:



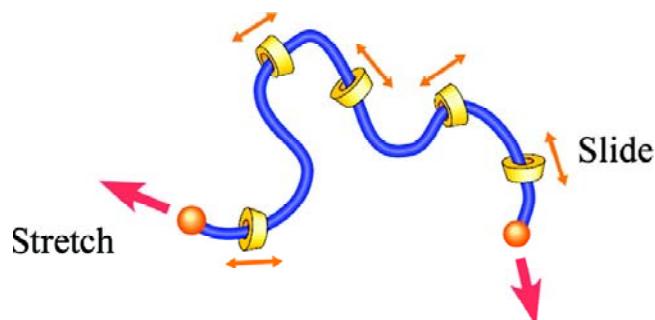
Amphiphilic block copolymers poly(ethylene oxide)-*b*-polystyrene (PEO-PS-Br) with various molecular weights and poly(ethylene oxide) homopolymer (PEO-Br) were synthesized and used as macroinitiators and stabilizers (reactive “surfactants”) for activator generated by electron transfer atom transfer radical polymerization (AGET ATRP) of *n*-butyl acrylate (BA), in miniemulsion either with or without ethyl 2-bromoisobutyrate (EBiB) as co-initiator. Under both conditions, the reactions were well controlled and stable latexes were formed. In the absence of EBiB, polymer particles with diameter around 120-230 nm were obtained, and the particles contained polymers with molecular weight M_n) 16 000-25 000 g/mol and relatively low polydispersity (M_w/M_n) 1.2-1.4). In the presence of a low molecular weight initiator, EBiB, the amount of surfactant used can be reduced in the reaction (1.7-4 wt % vs monomer). The percent of initiating sites from EBiB was changed from 30% to 90%, and the majority of the obtained polymers were initiated by EBiB. Nevertheless, because of the covalent linking of the surfactants to polymer chains, no free surfactant was left in the reaction system. The final diameter of latexes stabilized by reactive surfactants was around 200-390 nm, the number-average molecular weight M_n of the polymers obtained was 10 000-25 000 g/mol, and the polydispersity index was around 1.2.

- Concentration-Induced Conformational Change in Linear Polymer Threaded into Cyclic Molecules.

Mayumi, K.; Osaka, N.; Endo, H.; Yokoyama, H.; Sakai, Y.; Shibayama, M.; Ito, K. *Macromolecules* **2008**, *41*, 6480-6485.

12

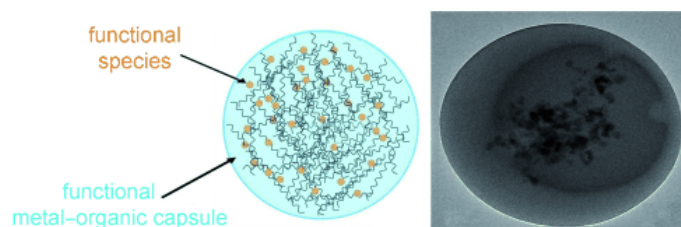
Abstract:



The concentration-induced conformational change in hydroxypropylated polyrotaxane (H-PR) composed of poly(ethylene glycol) (PEG) and hydroxypropylated R-cyclodextrins (CDs) was investigated at various concentrations from the overlap concentration c^* to the semidilute regime by using the small-angle neutron scattering technique. We employed the generalized Zimm plot with the wormlike chain model to analyze the scattering functions of H-PR since they deviated from the Ornstein-Zernike equation particularly in the high- Q range. It was found that the persistence length of H-PR decreased with increasing polymer concentration c_p , while those of PEG remained unchanged in the same molar concentration regime. This unusual concentration dependence of polymer conformation for H-PR may indicate that CDs in H-PR could slide freely and rapidly over the whole range of PEG chains in the neighborhood of c^* , but their mobility was suppressed as c_p increased due to some molecular interaction among CDs.

- Coordination Polymers: From Metal–Organic Frameworks to Spheres
Champness, N. R. *Angew. Chem. Int. Ed.* **2009**, *48*, 2274 – 2275.

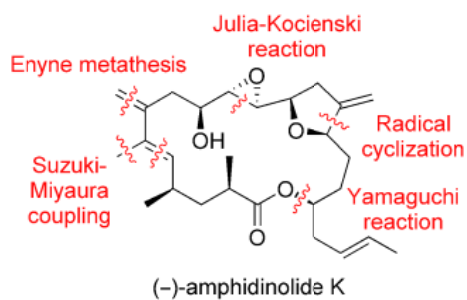
Abstract:



Sphere of destiny: Metal-organic spheres with remarkable encapsulation properties are readily prepared and their ability to host a wide range of guest species, including nanoparticles, fluorescent dyes, and quantum dots, is demonstrated. Both the metal-organic spheres and the encapsulated species maintain their fluorescent or magnetic properties, highlighting the importance of these systems as new multifunctional materials.

- Total Synthesis of (-)-Amphidinolide K
Ko, H. M.; Lee, C. W.; Kwon, H. K.; Chung, H. S.; Choi, S. Y.; Chung, Y. K.; Lee, E. *Angew. Chem. Int. Ed.* **2009**, *48*, 2364 – 2366.

Abstract:



Macrolide magic: An enyne cross-metathesis reaction of an alkynyl boronate with an alkene derivative as well as a radical cyclization reaction of a homopropargylic β -alkoxyacrylate are the key transformations in the total synthesis of the cytotoxic macrolide (-)-amphidinolide K.